

Title	Surface Phase Transitions in Two Dimensions: Metastability and Reentrance
Creators	Patrick, A. E. and Upton, P. J.
Date	1996
Citation	Patrick, A. E. and Upton, P. J. (1996) Surface Phase Transitions in Two Dimensions: Metastability and Reentrance. (Preprint)
URL	<a href="https://dair.dias.ie/id/eprint/662/">https://dair.dias.ie/id/eprint/662/</a>
DOI	DIAS-STP-96-08

## Surface Phase Transitions in Two Dimensions: Metastability and Re-entrance

A.E. Patrick<sup>1</sup> and P.J. Upton<sup>1,2</sup>

**Abstract.** A two-dimensional Ising model on an infinite strip is studied with boundary conditions inducing a long contour with its end points rooted to one edge. A surface field acts along the other edge. When an appropriate thermodynamic limit is taken, the model supports three *macroscopic* phases specified, apart from the value of the spontaneous magnetization, by the shape of the long contour on a macroscopic scale. Phase re-entrance is found as well as metastability. Simple entropic arguments are given which illuminate the origin of this re-entrance and suggest that this phenomenon is common for a wide class of models.

PACS numbers: 05.50.+q, 64.60.My, 68.45.Gd, 05.70.Fh.

---

<sup>1</sup>School of Theoretical Physics, Dublin Institute for Advanced Studies, 10 Burlington Road, Dublin 4, Ireland.

<sup>2</sup>H.H. Wills Physics Laboratory, University of Bristol, Tyndall Ave., Bristol, BS8 1TL, England.

A surface wetting transition occurs when one thermodynamic phase, which coexists in the bulk with at least one other phase, gets preferentially adsorbed against a wall (i.e., the substrate) until it forms a macroscopically thick layer. If the adsorbed phase is in the form of a sessile drop lying on the substrate with a contact angle of  $\vartheta$  then the wetting transition would correspond to having  $\vartheta \searrow 0$ ; the substrate being non-wet (or partially wet) when  $\vartheta > 0$  and (completely) wet when  $\vartheta = 0$ . Such a transition is an example of a surface phase transition which manifests itself as a singularity in a surface (excess) free energy. Cahn [1] predicted the existence of (first order) surface wetting transitions using squared-gradient Landau theory. A few years later Abraham [2] was able to show, through an exact solution, that a two-dimensional Ising model supports a second-order wetting transition (i.e.,  $\vartheta \searrow 0$  continuously). In this paper we demonstrate, on the basis of *exact* results, that a two-dimensional Ising model can also support a class of surface phase transitions related to wetting but are first order in that the contact angle jumps discontinuously. Such a model, got from applying appropriate boundary conditions with the thermodynamic limit taken in a particular way, describes a domain wall (or grand canonical sessile drop) with both its end points attached to one edge of an infinite strip with a pinning substrate on the opposite edge. A surprisingly rich variety of phase diagrams are found with some striking features including *phase re-entrance*.

The model is defined as follows. Ising spins  $\sigma_{x,y}$  taking values  $\pm 1$  are placed on sites  $(x,y) \in \Lambda \subset \mathbb{Z}^2$  of a square lattice wrapped around a cylinder with a circumference of  $M$  sites and a height of  $N$  sites. The spins interact through the following ferromagnetic nearest-neighbour Ising Hamiltonian

$$\mathcal{H}_{M,N}\{\sigma\} = -J_1 \sum_{x=1}^M \sum_{y=1}^{N-1} \sigma_{x,y} \sigma_{x,y+1} - J_2 \sum_{x=1}^M \sum_{y=1}^N \sigma_{x,y} \sigma_{x+1,y} - H_1 \sum_{x=1}^M \sigma_{x,1} \quad (1)$$

with  $\sigma_{M+1,y} = \sigma_{1,y}$  for all  $1 \leq y \leq N$ . Along the top edge of the cylinder ( $y = N$ ), two different boundary conditions,  $\mathcal{B}$ , are considered: (a)  $\mathcal{B} = ++$ , denoting the case where  $\sigma_{x,N} = +1$  for all  $x$ ; and (b)  $\mathcal{B} = +-$ , for the case where  $\sigma_{x,N} = -1$  for  $1 \leq x \leq L$  and  $\sigma_{x,N} = +1$  otherwise. The surface field,  $H_1$ , acting along  $y = 1$  is equivalent to adding an extra row of fixed spins along  $y = 0$ ,  $\{\sigma_{x,0} = +1\}_{x=1}^M$ , coupled to  $\{\sigma_{x,1}\}_{x=1}^M$  by vertical bonds of strength  $J_0 = H_1$  [2] and in what follows we use a contour representation where a contour is drawn between two nearest-neighbour sites containing antiparallel spins regardless of the sign of the coupling between them.

Fig. 1 shows some typical configurations of contours (generated by a Glauber-dynamics simulation) for the case with  $\mathcal{B} = +-$ . Here a domain wall (long contour) is induced at the top edge of the cylinder going from  $(\frac{1}{2}, N + \frac{1}{2})$  to  $(L + \frac{1}{2}, N + \frac{1}{2})$ . If  $H_1$  is sufficiently high the long contour will stay at a distance of order  $\sqrt{L}$  from the top edge as in Fig. 1(a). As  $H_1$  reduces, the long contour will tend to stick to the bottom edge since the lower  $H_1$  is, the greater the tendency for  $\sigma_{x,1} = -1$ . Eventually it will “pin” to the bottom edge making, in the macroscopic scale, a contact angle of  $\vartheta$  with  $y = 1$ . Fig. 1(b) shows the case where  $\vartheta < \pi/2$  (we must

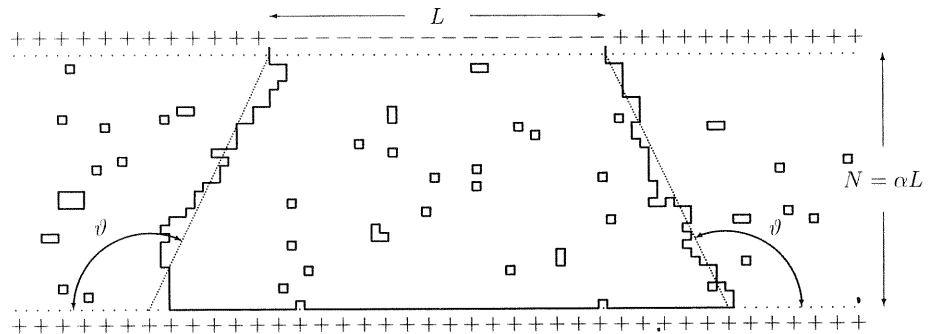


Figure 1c.

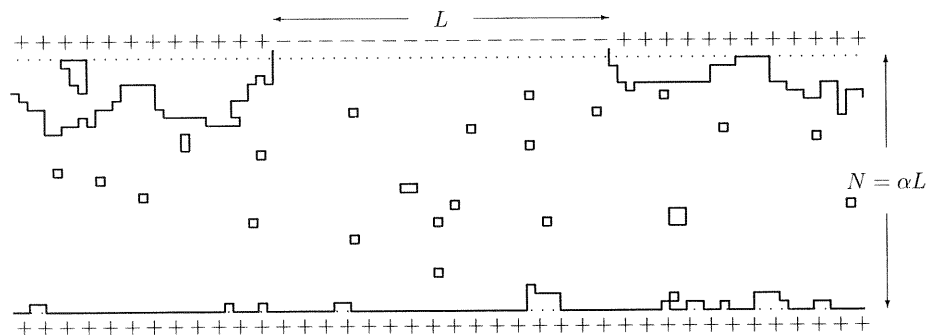


Figure 1d.

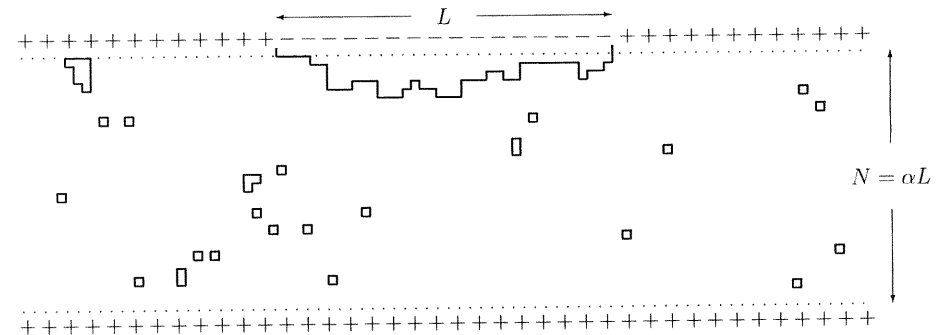


Figure 1a.

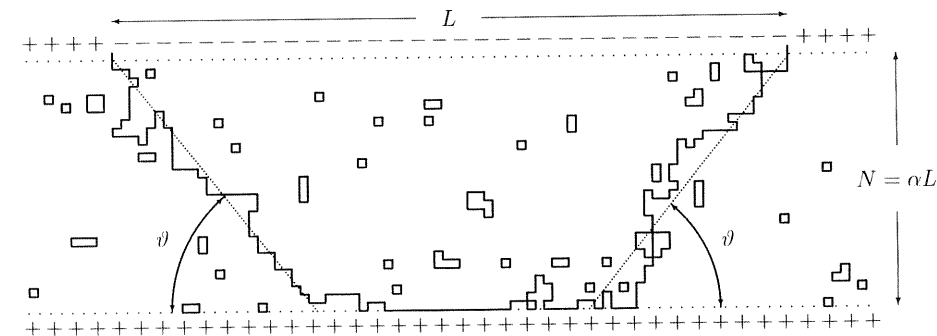


Figure 1b.

Figure 1.

Typical configurations (generated by a Glauber-dynamics simulation) for various values of  $T$  and the model parameters. (a) corresponds to Phase I; (b) and (c) correspond to Phase II for  $h > 0$  and  $h < 0$  respectively; and (d) corresponds to Phase III.

have  $\tan \vartheta > 2\alpha$  with  $N = \alpha L$  occurring when  $H_1 > 0$  and Fig. 1(c) the case with  $\pi/2 < \vartheta < \pi$  for  $H_1 < 0$ . As  $H_1$  continues to go sufficiently negative,  $\vartheta \nearrow \pi$  so that the long contour eventually spreads all over the bottom edge, and breaks into three pieces, with configurations exemplified by Fig. 1(d).

For each boundary condition  $\mathcal{B}$ , the canonical partition function  $Z_{\mathcal{B}} = \sum_{\{\sigma\}} \exp(-\beta \mathcal{H}_{M,N})$  is evaluated using exact methods [2]–[4] where  $\beta$  is the usual inverse temperature  $1/k_B T$ . The incremental free energy due to the presence of the domain wall is given by

$$f_{N,L}^{\times} = -\frac{k_B T}{L} \lim_{M \rightarrow \infty} \ln(Z_{+-}/Z_{++}). \quad (2)$$

In order to get a phase transition, further limits are required. If in (2) we take  $N \rightarrow \infty$  *before*  $L \rightarrow \infty$  there will be no additional phase transitions below bulk criticality. On the other hand, if  $L \rightarrow \infty$  is taken *before*  $N \rightarrow \infty$  one will obtain the second-order wetting transition of Abraham [2]. The crucial feature of our model is that  $N$  and  $L$  are kept at the same order as their limits are taken simultaneously. That is we set  $N = [\alpha L]$ , introducing the “shape ratio”  $\alpha$ , and then take  $L \rightarrow \infty$ . Thus we seek to determine

$$f^{\times}(T, h|\alpha, J_1, J_2) = \lim_{L \rightarrow \infty} f_{[\alpha L], L}^{\times}, \quad (3)$$

where  $h = H_1/J_1$ .

Equation (2) is evaluated using well established techniques reported elsewhere [2]–[4]. Here we just give a brief outline. The transfer matrix operates along the cylinder axis and is diagonalized using fermionic methods [5]. Along the top edge ( $y = N$ ), the  $\mathcal{B} = ++$  boundary condition is handled by being able to represent the corresponding final state,  $\langle +|$ , of the transfer operation in terms of fermionic vacuum states [6]. To get  $\mathcal{B} = +-$ , one applies a “block rotation” operator to  $\langle +|$  which has the effect of flipping those spins having  $1 \leq x \leq L$  and such an operator can be expressed as a bilinear form of fermionic creation and annihilation operators [6]. In order to deal with the other end of the cylinder one exploits the equivalence of the surface field acting on the bottom edge ( $y = 1$ ) with the additional row of fixed spins along  $y = 0$ . However, one needs to treat  $h > 0$  differently from  $h < 0$ . In both cases the modified coupling constant for the vertical bonds between  $y = 0$  and  $y = 1$  is set to be  $|h| J_1$  but for  $h > 0$ , *all* the spins along  $y = 0$  are kept up so that the initial state of the transfer operation is simply  $|+\rangle$ . For  $h < 0$ , one applies block-rotation operator to  $|+\rangle$  which flips the spins having  $-s \leq x \leq s$  and then we take the limit  $s \rightarrow \infty$  after first taking  $M \rightarrow \infty$ .

We first proceed to present the exact results for the case when  $h > 0$  as follows. Defining  $K_j = \beta J_j$  ( $j = 1, 2$ ), we find

$$\lim_{M \rightarrow \infty} Z_{+-}/Z_{++} = I_{N,L}(h) \quad (4)$$

where

$$I_{N,L}(h) = \frac{e^{2K_2}}{2\pi i} \int_{-\pi}^{\pi} d\omega \tan(\delta^*(\omega)/2) e^{iL\omega} \quad (5)$$

$$\times \frac{e^{\gamma(\omega)} - w(h) - [e^{-\gamma(\omega)} - w(h)] e^{-2N\gamma(\omega)}}{e^{\gamma(\omega)} - w(h) + [e^{-\gamma(\omega)} - w(h)] \tan^2(\delta^*(\omega)/2) e^{-2N\gamma(\omega)}}$$

with

$$w(h) = e^{2K_2} (\cosh 2K_1 - \cosh 2hK_1) / \sinh 2K_1. \quad (6)$$

The Onsager functions [7] contained in (5) are given by

$$\cosh \gamma(\omega) = \cosh 2K_1^* \cosh 2K_2 - \sinh 2K_1^* \sinh 2K_2 \cos \omega \quad (7)$$

$$e^{i\delta^*(\omega)} = \left[ (e^{i\omega} - A) (Be^{i\omega} - 1) / (Ae^{i\omega} - 1) (e^{i\omega} - B) \right]^{1/2} \quad (8)$$

where  $A = \exp 2(K_1 + K_2^*)$ ,  $B = \exp 2(K_1 - K_2^*)$  and the dual couplings are defined through  $\exp(-2K_j^*) = \tanh K_j$  ( $j = 1, 2$ ). In order to proceed with the large  $L$  asymptotics of the integral in (5), we examine the poles of the integrand given by the zeros of its denominator. The root equation for these zeros can be written as a polynomial of degree  $2N + 4$  in the variable  $\exp[-\gamma(\omega)]$ . This leads to  $2N + 4$  simple zeros in the denominator, four of which are also zeros of the numerator. Thus we find that the integrand in (5) has  $2N$  poles (along the imaginary axis) given by  $\omega = \pm iv_j$  ( $j = 1, \dots, N$ ) where, for all real  $w(h)$ ,  $\hat{\gamma}(0) < v_2 < \dots < v_N < \hat{\gamma}(\pi)$ . Here,  $\hat{\gamma}(\omega)$  is the same as  $\gamma(\omega)$  given by (7) except that  $K_1$  and  $K_2$  are interchanged so that  $\hat{\gamma}(0) = 2(K_1 - K_2^*)$ . Now, for  $w(h) < 1$  we have  $\hat{\gamma}(0) < v_1 < v_2$  whereas for  $w(h) > 1$  it turns out that  $0 < v_1 < \hat{\gamma}(0)$ . In the latter case we find that  $\gamma(iv_1) \sim \ln w(h)$  as  $N \rightarrow \infty$ . By deforming the contour of integration in (5) around the poles in the upper-half plane, it follows that for  $w(h) > 1$  we can write  $I_{[\alpha L], L}(h) = R_1(L) + R_2(L)$  such that as  $L \rightarrow \infty$

$$R_1(L) \sim c_1(T, h) [w(h)]^{-2\alpha L} e^{-v(h)L} \quad (9)$$

$$R_2(L) \sim c_2(T) L^{-3/2} e^{-L\hat{\gamma}(0)} \quad (10)$$

where  $R_1(L)$  comes from the residue of the single isolated pole at  $\omega = iv_1$  whilst  $R_2(L)$  is the contribution from the “band” of poles forming a cut along  $\hat{\gamma}(0) < \text{Im } \omega < \hat{\gamma}(\pi)$  as  $L \rightarrow \infty$ . Also,  $v(h) = \lim_{L \rightarrow \infty} v_1$  which is given by  $\gamma[iv(h)] = \ln w(h)$ , or equivalently  $v(h) = \hat{\gamma}[i \ln w(h)]$ . When  $w(h) < 1$ , only the second term will contribute so that  $I_{[\alpha L], L}(h) \sim R_2(L)$  as  $L \rightarrow \infty$ . Hence from (2), (3), (4), (9) and (10) we have

$$\beta f^\times(T, h | \alpha, J_1, J_2) = \begin{cases} \min[2\alpha \ln w(h) + v(h), \hat{\gamma}(0)] & \text{for } w(h) > 1; \\ \hat{\gamma}(0) & \text{for } w(h) < 1; \end{cases} \quad (11)$$

and one should recall that  $\hat{\gamma}(0) = 2(K_1 - K_2^*)$ .

We now present the results for  $h < 0$ . Following the procedure outlined earlier, one obtains, after putting  $N = [\alpha L]$ ,

$$\lim_{M \rightarrow \infty} Z_{+-}/Z_{++} = I_{[\alpha L], L}(|h|) + R_3(L) \quad (12)$$

where as  $L \rightarrow \infty$

$$R_3(L) \sim c_3(T, h) [w(h)]^{-2\alpha L} e^{+v_1(|h|)L} \quad (13)$$

with  $I_{N,L}(|h|)$  being that given by (5) and, also as before,  $v_1(|h|)$  is such that

$$\lim_{L \rightarrow \infty} v_1 = v(|h|) = \hat{\gamma}[i \ln w(h)]$$

for  $w(h) > 1$  while  $\lim_{L \rightarrow \infty} v_1 = \hat{\gamma}(0)$  for  $w(h) < 1$ . Hence, putting (12) and (13) into (2) and (3), one obtains

$$\beta f^\times(T, h|\alpha, J_1, J_2) = \begin{cases} \min[2\alpha \ln w(h) - v(|h|), \hat{\gamma}(0)] & \text{for } w(h) > 1; \\ -\hat{\gamma}(0) & \text{for } w(h) < 1. \end{cases} \quad (14)$$

Note that  $-v(|h|)$  is the analytical continuation of  $v(h)$  through to negative  $h$  so that, in general,  $f^\times(T, h)$  is analytic at  $h = 0$  (since  $w(0) > 1$  for all  $T < T_c$ ).

Now that we have  $f^\times(T, h|\alpha, J_1, J_2)$  for all  $T \leq T_c$  and  $h \in (-\infty, \infty)$  the complete phase diagram can be determined. Firstly, it is clear from (11) and (14) that a first-order phase transition occurs at  $h = h_\sigma(T)$  for  $T < T_c$  where  $h_\sigma(T)$  is implicitly given by

$$2\alpha \ln w(h_\sigma) + v(h_\sigma) = \hat{\gamma}(0) \quad (15)$$

and it is understood that  $v(h_\sigma) = -v(|h_\sigma|)$  for  $h_\sigma < 0$ . Secondly, one finds a critical wetting transition at  $h = h_w(T) < 0$  where  $w(h_w) = 1$ , which is the condition for the wetting transition of Abraham type [2] (although in our case this occurs at negative  $h$ ), and one can see that  $h_w(T) < h_\sigma(T)$  for all  $T < T_c$ . Phase diagrams for various values of  $\alpha$ ,  $J_1$  and  $J_2$  are plotted in Fig. 2. For  $T < T_c$ , there are three distinct macroscopic phases (i.e., locations of the long contour at the macroscopic scale). Phase I, occurring when  $h > h_\sigma(T)$ , is characterized by having the long contour close to the top edge, at a distance of order  $\sqrt{L}$  from it. A typical configuration is shown in Fig. 1(a). Phase II, occurring when  $h_w(T) < h < h_\sigma(T)$ , has the long contour “pinned” to the bottom edge with a contact angle of  $\vartheta$  where  $\vartheta < \pi/2$  for  $h > 0$  [Fig. 1(b)] and  $\pi/2 < \vartheta < \pi$  for  $h < 0$  [Fig. 1(c)]. The sloping part of the domain wall fluctuates on a scale of  $\sqrt{L}$  about its mean position as it crosses from the top to the bottom edge. We stress again that the transition between Phases I and II is *first order* since  $\vartheta$  (order parameter) changes discontinuously at  $h = h_\sigma(T)$  (setting  $\vartheta = 0$  for the horizontal position of the interface in Phase I) whereas when  $h \searrow h_w(T)$  one has  $\vartheta \nearrow \pi$  continuously, this last being the critical wetting transition of the type found by Abraham [2]. Thus, for  $h < h_w(T)$  we encounter Phase III where one finds the negatively magnetized Gibbs states spread all over the lower half of the strip and the long contour split into three pieces, as typified in Fig. 1(d). We now make the following remarks:

(i) If we denote  $f_\Phi^\times(T, h)$  as the incremental free energy for the Phase  $\Phi$  ( $\Phi = \text{I, II, III}$ ), see Eq. (3), then clearly Eqs. (11) and (14) yield  $\beta f_\text{I}^\times(T) = \hat{\gamma}(0) = 2(K_1 - K_2^*)$  (which is just the interfacial tension in units of  $k_B T$  for a free interface running parallel to the edges);  $\beta f_\text{II}^\times(T, h) = 2\alpha \ln w(h) + v(h)$ ; and  $\beta f_\text{III}^\times(T) = -\hat{\gamma}(0)$ . These expressions, and therefore Eq. (15), could have been anticipated through the Wulff

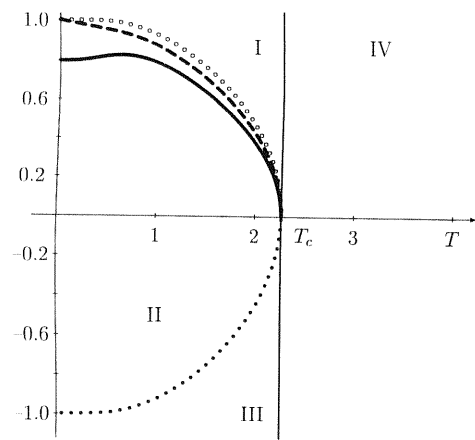


Figure 2a.

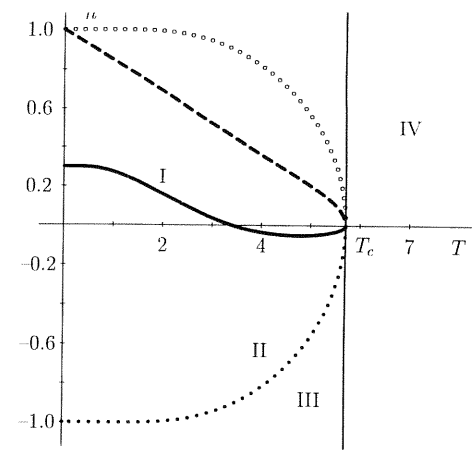


Figure 2c

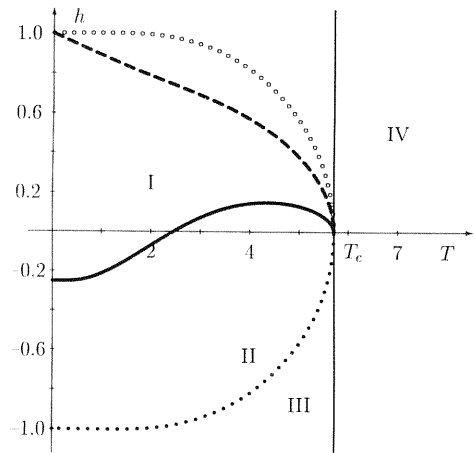


Figure 2b.

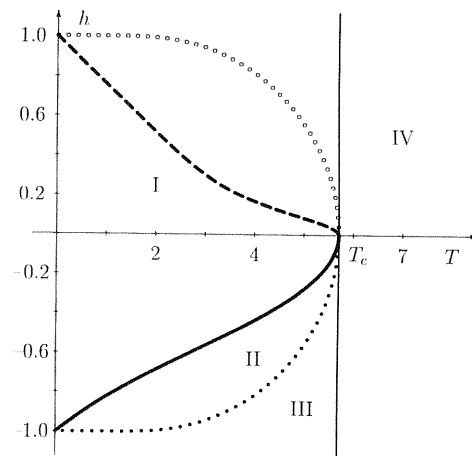


Figure 2d.

Figure 2.

A selection of phase diagrams showing three phase boundaries. The phase boundary separating Phases I and II is depicted by the *unbroken* bold curve and that between Phases II and III by the *black* dots. The usual bulk critical transition (at  $T = T_c$ ) is depicted by the unbroken vertical line to the right of which is the supercritical Phase IV. The curve  $h = h_s(T)$ , i.e., the *metastability limit*, is depicted by the *broken* bold curve and the *white* dots depict the Abraham transition [2] (occurring when  $L \rightarrow \infty$  is taken *before* taking  $N \rightarrow \infty$ ). The parameter values are (a)  $\alpha = 0.1$ ,  $J_1 = J_2 = 1$ ; (b)  $\alpha = 0.125$ ,  $J_1 = 1$ ,  $J_2 = 5$ ; (c)  $\alpha = 1.75$ ,  $J_1 = 5$ ,  $J_2 = 1$ ;



construction [8], i.e. minimizing the domain-wall free energy w.r.t the shape of the domain. Indeed, the long contour in Phase II consists of a pinned horizontal part and two inclined symmetric parts, making an angle  $\theta$  with the attracting bottom edge. The length of the pinned part is  $L(1 - 2\alpha \cot \theta)$  and the incremental free energy of the pinned interface per unit length is  $\beta\tau_p = v(h)$ . The length of each inclined part is  $\alpha L / \sin \theta$  with an interfacial tension per unit length (in units of  $\beta^{-1}$ ) given by  $\tau(\theta) = [\gamma(\omega_0) - i\omega_0 \cot \theta] \sin \theta$ , see [9], where  $\omega_0 = \omega_0(\theta)$  is a solution of

$$\gamma'(\omega) = i \cot \theta. \quad (16)$$

Therefore the incremental free energy of Phase II with the contact angle  $\theta$ ,  $F^\times(\theta)$ , is given by

$$\beta L F^\times(\theta) = L(1 - 2\alpha \cot \theta)v(h) + 2\alpha L \tau(\theta) \csc \theta. \quad (17)$$

The value of  $\theta$  minimizing  $F^\times(\theta)$  — the contact angle  $\vartheta$  — is given implicitly by  $\omega_0(\theta) = iv(h)$ . Differentiating (7) w.r.t.  $\omega$  and using (16) together with  $\gamma(\omega_0(\theta)) = \gamma[iv(h)] = \ln w(h)$  one obtains the expression previously derived in [3] and [10]

$$\tan \vartheta = \frac{\sinh \ln w(h)}{[\cosh \gamma(0) - \cosh \ln w(h)]^{1/2} [\cosh \gamma(\pi) - \cosh \ln w(h)]^{1/2}}. \quad (18)$$

The minimum of  $\beta F^\times(\theta)$  is given by

$$\beta F^\times(\vartheta) = 2\alpha \ln w(h) + v(h), \quad (19)$$

which coincides with  $\beta f_{\text{II}}^\times(T, h)$  as required. The expression for  $\beta f_{\text{III}}^\times(T, h)$  is intuitively obvious as well. The long contour for the boundary condition  $\mathcal{B} = ++$  and  $w(|h|) < 1$  consists of two nearly horizontal (in the scale  $O(L)$ ) pieces. One pinned to the bottom row and the other one hanging somewhere in the bulk. In the case where  $\mathcal{B} = +-$  the long contour consists of three pieces (nearly horizontal in the scale  $O(L)$ ) one pinned at the bottom row (exactly the same as the pinned piece in the case  $\mathcal{B} = ++$ ) and two fluctuating pieces (see Fig. 1(d)) with a total length *less* by  $L$  compared to the length of the unpinned piece in the  $\mathcal{B} = ++$  case (in the “incremental” sense). Since the incremental free energy per unit length of the free interface is  $\hat{\gamma}(0)$ , it is clear that

$$\beta f_{\text{III}}^\times(T, h) = -\hat{\gamma}(0). \quad (20)$$

One can also follow Ref. [3] and check the mean shape of the domain wall by examining the expectation for the bond energy  $\sigma_{x,y}\sigma_{x+1,y}$ , thus explicitly confirming the character of the various phases as described above.

(ii) A comprehensive macroscopic description of the model (1) requires two characteristics: the absolute value of the spontaneous magnetization and the shape of the domain wall separating regions with magnetizations of opposing sign (which for given values of the parameters  $\beta, J_1, J_2, h, \alpha$  completely specify the macroscopic state of the system). For positive values of the surface field  $h$  the shape of the domain

wall in the macroscopic scale is a continuous function  $\varphi = f(\chi)$ ,  $f : [0, 1] \rightarrow [0, 1]$ , where  $\chi$  specifies a column of the lattice

$$c_\chi \equiv \{(x, y) : x = [\chi L]; y = 1, \dots, [\alpha L]\} \quad (21)$$

and  $\varphi$  gives the location of the domain wall  $y = [\varphi \alpha L]$  in that column. More complicated shapes of the domain wall have vanishingly small probabilities as  $L \rightarrow \infty$ . The Gibbs distribution corresponding to the Hamiltonian (1) induces a probability measure on the space of function  $f(\cdot)$ . The equilibrium (most probable) shape of the domain wall minimizes the total surface tension — the Wulff functional. The local minima of the total surface tension correspond to metastable shapes of the domain wall, that is, to metastable macroscopic states of the system. For the model under consideration it is possible to construct explicitly the Wulff functional and the large  $L$  asymptotic expansion for the probability measure on the space of functions  $f(\cdot)$ . It turns out that for positive values of the surface field there are at most two local minima: domain wall in the shape of the horizontal line at the top of the strip (Phase I), and domain wall in a trapezoid shape pinned to the bottom of the strip (Phase II). In this note we present only the results concerning the location of the domain wall in the column  $c_{1/2}$ . Consider the indicator function  $I(x, y) = (1 - \sigma_{x,y}\sigma_{x+1,y})/2$ , which is equal 1 if the sites  $(x, y)$  and  $(x + 1, y)$  are separated by a contour, and  $I(x, y) = 0$  otherwise. Note that the sites can be separated by the large contour as well as small contours, the latter possibility is often much more likely. To obtain an efficient approximation for the probability that the sites are separated by the large contour consider the function

$$P(x, y) = \langle I(x, y) \rangle_{+-} - \langle I(x, y) \rangle_{++}, \quad (22)$$

where  $\langle \cdot \rangle_{\mathcal{B}}$  is the canonical expectation with boundary conditions  $\mathcal{B}$ . It is believed that the probability for the sites  $(x, y)$  and  $(x + 1, y)$  to be separated by the long contour has the same order of magnitude as the function  $P(x, y)$ . Anticipating the exponential decay of the function  $P(x, y)$  we introduce the rate function

$$R(\chi, \varphi) = - \lim_{L \rightarrow \infty} L^{-1} \ln P([\chi L], [\varphi \alpha L]), \quad (23)$$

which should coincide with the rate function for the probability that the sites  $(x, y)$  and  $(x + 1, y)$  are separated by the long contour. This rate function was calculated exactly [11] with properties which we illustrate for the case of  $R(1/2, \varphi)$  (for  $h > 0$ ) by way of example. Note first of all that the geometry of our model gives the restriction  $\tan \vartheta(h) > 2\alpha$  for the possible values of the contact angle. Define  $h_s(T)$  through  $\tan \vartheta[h_s(T)] = 2\alpha$ . When  $0 < h < h_\sigma(T)$  the rate function was found to have a *global* minimum at  $\varphi = 0$  (that is, Phase II is stable) and a *local* minimum at  $\varphi = 1$  (Phase I is metastable). For  $h_\sigma(T) < h < h_s(T)$  the rate function has a global minimum at  $\varphi = 1$  (Phase I is stable) and a local minimum at  $\varphi = 0$  (Phase II is metastable). Finally, for  $h \geq h_s(T)$  the rate function has only *one* minimum at  $\varphi = 1$  (Phase I is stable, Phase II is absent). Of course, the rate function is zero at

its global minimum. One can obtain similar conclusions concerning the metastable states on the basis of analytical continuations (which exist for this model) of the incremental free energies  $f_I^\times(T)$  and  $f_{II}^\times(T, h)$  outside the domains of their definitions specified by the corresponding phase diagram. It is not clear, however, how far one could follow the analytic continuation and still be sure that the metastable states exist. A correctly chosen rate function provides a *precise* notion of metastability defined in terms of local (and non-global) minima of a rate function. A vaguely similar metastability and hysteresis phenomenon was studied by McCoy and Wu nearly 30 years ago [12]. They also identified metastable states on the basis of a rate function and analytic continuation. However, McCoy and Wu faced considerable difficulties in not being able to obtain a unique hysteresis loop, that is, in not being able to determine when the metastable states cease to exist. The main problem was the disappearance of the local minimum of the rate function corresponding to a metastable state much earlier than one would expect it. Somewhat later, in their book [13], McCoy and Wu identified the correct hysteresis loop and hinted that the previous problems with the rate function minima are due to an inappropriate choice of the rate function (which is extremely sensitive to, e.g., the boundary conditions imposed). We claim that a precise notion of metastability of the type considered in the present paper and in the papers by McCoy and Wu [12, 13] can always be defined in terms of local minima of a rate function. We hope to return to this question in a future publication.

(iii) The phase diagrams in Fig. 2 exhibit the phenomenon of phase *re-entrance* with regard to Phases I and II, namely, for a given (fixed) value of  $h$ , the macroscopic phase which is a small perturbation of the ground state is thermodynamically stable for low enough  $T$  whereas another phase becomes stable at a higher temperature  $T_1 > 0$  before the first phase becomes thermodynamically stable again at a yet higher temperature  $T_2 > T_1$ . In other words, there exists a range of  $h$  such that the equation  $h = h_\sigma(T)$  has two distinct solutions  $T = T_1$  and  $T = T_2$ . This effect is entropically driven although it might appear surprising that the (pinned) Phase II can stabilize at some higher temperature when Phase I is the ground state since one normally thinks of the pinned phase as having a lower entropy. That this is possible is due to the large entropic contributions coming from the sloping part of the long contour as it crosses from edge to edge in the case of Phase II. Indeed, the following simple argument can be used at low temperatures to predict this effect. Consider the case when  $h > 0$  (the argument can easily be adapted to cover the case  $h < 0$ ). The incremental ground state energy of Phase I (relative to the ground state of the system with  $++$  boundary conditions),  $E_I^\times$ , is given by  $E_I^\times = 2J_1L$  whereas for Phase II we have  $E_{II}^\times = (2hJ_1 + 4\alpha J_2)L$ . Hence  $h_\sigma(0) = 1 - 2\alpha J_2/J_1$ , which is positive provided  $2\alpha < J_1/J_2$ . In Phase II for  $T = 0$ , the long contour crosses  $y = 1$  at the contact points  $(\frac{1}{2}, 1)$  and  $(L + \frac{1}{2}, 1)$  with a contact angle of  $\pi/2$ . For temperatures slightly above zero we consider those configurations where the contact points are shifted to  $(\frac{1}{2} + x_0, 1)$  and  $(L + \frac{1}{2} - x_0, 1)$  with minimal cost in energy (i.e., the long contour crosses from one edge to the other through a monotonic staircase).

The partition-function ratio (4) is approximated by

$$\lim_{M \rightarrow \infty} Z_{+-}/Z_{++} \approx \sum_{x_0=0}^{L/2} W_{\text{II}}(x_0) e^{-\beta E_{\text{II}}^{\times}(x_0)} \quad (24)$$

where the incremental energy is

$$E_{\text{II}}^{\times}(x_0) = 4J_1 x_0 + (L - 2x_0)2hJ_1 + 4\alpha L J_2 \quad (25)$$

and  $W_{\text{II}}(x_0)$  is the number of corresponding configurations which is given by  $W_{\text{II}}(x_0) = [(\alpha L + x_0)!/(\alpha L)!x_0!]^2$ . At low temperatures, the summation in (24) is well approximated by its largest term. Hence it follows that

$$f_{\text{II}}^{\times}(T, h) \approx \lim_{L \rightarrow \infty} L^{-1} \min_{x_0} [E_{\text{II}}^{\times}(x_0) - k_{\text{B}} T \ln W_{\text{II}}(x_0)] \quad (26)$$

$$\approx 2hJ_1 + 4\alpha J_2 - 2\alpha k_{\text{B}} T e^{-(1-h)K_1} \quad (27)$$

as  $T \rightarrow 0$  and the corresponding contact angle given by  $\cot \vartheta = x_0/\alpha L \approx \exp[-2(1-h)K_1]$ . Now, when  $J_2 > (1-h)J_1$ , the exponential in (27) will dominate over the leading low-temperature correction to  $f_{\text{I}}^{\times} \approx 2J_1$  given by  $e^{-2K_2}$ . From this it follows that  $h_{\sigma}(T) - h_{\sigma}(0) \approx \alpha K_1^{-1} e^{-4\alpha K_2}$  as  $T \rightarrow 0$  thus causing Phase II to stabilize for  $T \in (T_1, T_2)$  even though Phase I is stable when the temperature is small enough. Since, on general grounds,  $\vartheta$  decreases as  $T$  increases, Phase I will eventually stabilize again at a higher  $T_2 < T_c$  thus completing the re-entrant effect. For  $J_2 > (1-h)J_1$ , (27) agrees with the leading temperature-dependent term of the low-temperature expansion of the exact expression for  $f_{\text{II}}^{\times}(T, h)$  as does the expression for  $\vartheta$ . This heuristic low-temperature entropic argument should hold for more general models and for higher dimensions.

(iv) Note that both  $h_{\sigma}(T)$ ,  $h_{\text{w}}(T) \rightarrow 0$  as  $T \nearrow T_c$ . If  $t = T_c - T$ , one finds that  $h_{\text{w}}(T) \sim -A_1 t^{1/2}$  as  $t \searrow 0$ , (here, and in what follows,  $A_1, A_2, \dots$  denote *positive* constants), as is usual for the Abraham transition [2]. If we denote  $K_1^c = J_1/k_{\text{B}}T_c$  then  $h_{\sigma}(T) \sim (\sinh 2K_1^c - 2\alpha) A_2 t^{1/2}$  as  $t \searrow 0$  provided  $\sinh 2K_1^c \neq 2\alpha$ . However, as one can see from Fig. 2, it is possible for  $h_{\sigma}(T)$  to pass through zero (linearly) at some temperature  $T_0 < T_c$ . This will happen when  $\hat{\gamma}(0) = 2\alpha\gamma(0)$  is satisfied. As  $T_0$  merges with  $T_c$ , occurring when  $\sinh 2K_1^c = 2\alpha$ ,  $h_{\sigma}(T)$  will show different behaviour near  $T_c$  given by  $h_{\sigma}(T) \sim [1 - (2\alpha J_2/J_1)^2] A_3 t^{3/2}$  as  $t \searrow 0$ .

To conclude, in this paper we have introduced an exactly solved model which exhibits a rich phase diagram containing three subcritical macroscopic phases characterized by the shape of a macroscopically large domain wall. A precise definition of metastability (involving a probabilistic rate function) was used to show that the model supports metastable phases. Phase re-entrance was also found and heuristic arguments indicate that this phenomenon would occur in more general (insoluble) models and at higher dimensions.

PJU acknowledges support from the Human Capital and Mobility Program of the European Union and the Engineering and Physical Science Research Council (United Kingdom) under grant number B/94/AF/1769.

## References

- [1] J.W. Cahn, *J. Chem. Phys.* **66**, 3667 (1977).
- [2] D.B. Abraham, *Phys. Rev. Lett.* **44**, 1165 (1980).
- [3] D.B. Abraham and L-F. Ko, *Phys. Rev. Lett.* **63**, 275 (1989).
- [4] D.B. Abraham, N.M. Švrakić, and P.J. Upton, *Phys. Rev. Lett.* **68**, 423 (1992).
- [5] T.D. Schultz, D.C. Mattis, and E.H. Lieb, *Rev. Mod. Phys.* **36**, 856 (1964).
- [6] D.B. Abraham and P. Reed, *Commun. Math. Phys.* **49**, 35 (1976).
- [7] L. Onsager, *Phys. Rev.* **65**, 117 (1944).
- [8] G. Wulff, *Z. Krystallogr. Mineral* **34**, 449 (1901).
- [9] D.B. Abraham and P. Reed, *J. Phys.* **A10**, L121 (1977).
- [10] D.B. Abraham, J. De Coninck, and F. Dunlop, *Phys. Rev.* **B39**, 4708 (1989).
- [11] A.E. Patrick and P.J. Upton (to be published).
- [12] B.M. McCoy and T.T. Wu, *Phys. Rev.* **162**, 436 (1967); **174**, 546 (1968).
- [13] B.M. McCoy and T.T. Wu, *The two-dimensional Ising model* (Harvard University Press, Cambridge, Mass., 1973).